



저작자표시-비영리-변경금지 2.0 대한민국

이용자는 아래의 조건을 따르는 경우에 한하여 자유롭게

- 이 저작물을 복제, 배포, 전송, 전시, 공연 및 방송할 수 있습니다.

다음과 같은 조건을 따라야 합니다:



저작자표시. 귀하는 원저작자를 표시하여야 합니다.



비영리. 귀하는 이 저작물을 영리 목적으로 이용할 수 없습니다.



변경금지. 귀하는 이 저작물을 개작, 변형 또는 가공할 수 없습니다.

- 귀하는, 이 저작물의 재이용이나 배포의 경우, 이 저작물에 적용된 이용허락조건을 명확하게 나타내어야 합니다.
- 저작권자로부터 별도의 허가를 받으면 이러한 조건들은 적용되지 않습니다.

저작권법에 따른 이용자의 권리는 위의 내용에 의하여 영향을 받지 않습니다.

이것은 [이용허락규약\(Legal Code\)](#)을 이해하기 쉽게 요약한 것입니다.

[Disclaimer](#)

**The radiomics approach of sialadenitis
using various imaging modality in
animal model**

Park Gun Chan

The Graduate School

Yonsei University

Department of Dentistry

**The radiomics approach of sialadenitis
using various imaging modality in
animal model**

Directed by Professor Chena Lee, D.D.S., Ph.D.

The Doctoral Dissertation submitted to the Department of
Dentistry, and the Graduate School of Yonsei University
in partial fulfillment of the requirements for the degree of
Doctor of Philosophy in Dental Science

Gun Chan Park

February 2022

This certifies that the Master's degree of
Gun Chan Park is approved.

Thesis Supervisor: **Prof. Chena Lee**

Thesis Committee Member: **Prof. Sang-Sun Han**

Thesis Committee Member: **Prof. Kug Jin Jeon**

The Graduate School

Yonsei University

February 2022

감사의 글

남들과 달리 가을에 들어와 두 해를 보내고 다시 가을이 훌쩍 지나 늦게나마 감사의 글을 씁니다. 작은 치과의 치과의사로, 한 가정의 아버지로, 대학원의 학생으로 여러 개의 역할을 하며, 문득 드는 생각은 어느 하나 오롯이 홀로 하는 역할이 없다는 것입니다. 나를 도와주는 직원들이 없었다면, 아내와 아이의 도움이 없었다면, 여러 교수님 및 동료 분들의 도움이 없었다면, 단 하나의 역할이라도 제대로 할 수 있었을까요? 새삼, 저의 곁을 지켜주시는 많은 분들에게 감사한 마음이 듭니다. 특히, 공부하는 학생으로서의 역할에 충실할 수 있도록 많은 도움을 주신 한상선 교수님과 전국진 교수님께 감사드리고, 저의 지도교수님이신 이채나 교수님께 깊은 감사드립니다. 이채나 교수님의 도움이 계셨기에 논문을 무사히 마무리할 수 있었습니다. 제가 어려움에 힘들어할 때면 언제나 곁에서 도와주셨습니다. 또한, 김영현 선생님과 이아리 선생님께도 감사의 마음을 전하고 싶습니다. 저에게는 천국만마로 느껴질 정도로 든든한 조력자입니다. 늘 열린 마음으로 도와주셔서 감사합니다.

대학교에서 졸업하고 수련하고 봉직의로 수련의로 쉼 없이 달려가다

조금은 지쳐갈 때쯤, 새롭고, 깊은 영역의 공부를 할 수 있어서 좋았습니다.
또, 고갈된 에너지를 채우는 것에 넘어서 새로운 에너지를 더 충전할 수
있어서 너무나 좋았습니다. 일상에 젖어있는 루틴에서 잠시 빠져나오는
것으로 좀더 다른 위치에서 저의 일상을 바라볼 수 있어서 좋았습니다.
저에게는 너무나도 고맙고 감사한 시간들이었습니다. 다시 한번 나의 역할에
충실할 수 있도록 도와주신 여러분들에게 감사드립니다.

끝으로 사랑하는 아내와 나의 분신 아들에게도 사랑한다는 말을 전합니다.
저에게 간신히 찾아낸 나의 삶의 과정이며 목표이며 결과입니다. 사랑합니다.

2021년 12월 저자 씀

TABLE OF CONTENTS

TABLE OF CONTENTS	i
LIST OF TABLES	ii
LIST OF FIGURES	iii
ABSTRACT	iv
I. INTRODUCTION.....	1
II. MATERIALS AND METHODS.....	5
III. RESULTS	13
IV. DISCUSSION	23
V. CONCLUSION	29
REFERENCES	30
ABSTRACT (in Korean).....	33

LIST OF TABLES

Table 1. Specification of unit and imaging condition according to the imaging modality.....	8
Table 2. Overall radiomics features analyzed.....	14
Table 3. Radiomics feature consistent with gland state.....	17

LIST OF FIGURES

Figure 1. Schematic workflow of overall experiment.....	5
Figure 2. Surgical simulation of sialadenitis.....	6
Figure 3. Representative image of computed tomography, magnetic resonance imaging and ultrasonography.....	10
Figure 4. Histology of normal, transient and chronic sialadenitis.....	11
Figure 5. Region of Interest (ROI) selection.....	13
Figure 6. Radiomics features selected in computed tomography.....	18-20
Figure 7. Radiomics features selected in magnetic resonance imaging.....	21-22
Figure 8. Radiomics features selected in ultrasonography.....	23

Abstract

The radiomics approach of sialadenitis using
various imaging modality in animal model

Park Gun Chan

Department of Dentistry

The Graduate School, Yonsei University

(Directed by Professor Chena Lee, D.D.S., PhD.)

Purpose: This study was to establish reliable radiomics feature in computed tomography (CT), magnetic resonance imaging (MRI) and ultrasonography (US) for diagnosis of sialadenitis induced in rat model.

Materials and Methods: Seven-week, 350-400g weighted wister strain rats were divided into experimental (n=7) and control (n=8) groups. For all subjects, contrast enhanced-computed tomography (CECT), T2-weighted MRI, and US were obtained. After the imaging examination, control subjects were sacrificed and submandibular glands were extirpated. For the experimental subjects, left submandibular glands were exposed to induced transient sialadenitis, and the right gland was ligated to induce chronic sialadenitis. After 2 weeks from the surgery, the same imaging examinations, CECT, MRI, and US, were performed. Then the experimental subjects were also sacrificed to extract the gland.

Observation of all images was conducted through visual diagnosis and histological diagnosis of extracted glands, and through this, it was identified in three categories (normal, transient, chronic sialadenitis).

For radiomics analysis, region of interest (ROI) was determined following the border of submandibular gland in CECT, MRI and US. The values of 50 radiomics features were obtained using LIFEx software. Then the features consistent with visual diagnosis were selected.

All radiomics values according to the gland state were compared using Kruskal willis test with 95% confidential interval. Post-hoc analysis was performed using Bonferroni test.

Results: There were 13 radiomics features showing statistical difference among gland status in CECT. All 13 features showed statistical significant differences between normal and chronic sialadenitis ($P < 0.05$). For MRI, 9 features were selected, and they showed statistical significant difference between normal and chronic sialadenitis gland. Three radiomics features were selected in US, showing differences between normal and chronic sialadenitis while one of which also showed differences between transient and chronic sialadenitis.

Conclusions: All imaging modality, CECT, MRI and US showed radiomics features consistent with visual diagnosis. This suggests that radiomics characteristics can be useful for recognizing the progression stage of sialadenitis based on the objective values.

Keywords: Radiomics, Sialadenitis, Computed tomography, Magnetic resonance imaging, Ultrasonography

The radiomics approach of sialadenitis using various
imaging modality in animal model

Gun Chan Park

Department of Dentistry

The Graduate School, Yonsei University

(Directed by Professor Chena Lee, D.D.S., PhD.)

I. INTRODUCTION

The salivary glands are mainly composed of adipose and fibrous tissues, typically intestinal, mucous and myoepithelial cells, and ducts consist of small to intermediate, striated, and secretory ducts. ¹

Salivary gland diseases can be caused by a variety of causes, including trauma, surgery, and radiation. Partial closure of the duct also may cause

chronic salivary inflammation, due to reverse infection from low saliva flow. Continuous duct obstruction also may cause irreversible destruction of gland tissue and eventually require a total resection of the gland.²

For the current evaluation of inflammatory changes of the gland, sialadenitis can be diagnosed through computed tomography (CT) or magnetic resonance imaging (MR). However, with those imaging modalities, periodic inspections are difficult given the problems such as cost or radiation exposure. In addition, diagnosing sialadenitis by recognizing high or low attenuation in CT or high and low signal intensity in MR imaging is clinician's subjective decision. Ultrasonography (US) is another choice of modality which is relatively easy to perform and non-radiation diagnostic tool. In US, it is known that normal salivary gland shows uniform echo while pathologic gland shows heterogenous echo. However, the criteria for diagnosis of sialadenitis in US is not clearly established and not specific enough.³

As such, imaging is heavily dependent on the experience or subjective impression of the clinician to diagnose. High and low attenuation in CT

image, intensity of signal in MRI, or heterogeneity of echoes in US all correspond to a clinician's subjective decision rather than an objective value. Thus, there has been constant demand for quantitative evaluation criteria in the field of diagnostic imaging. Radiomics, a quantitative approach to medical imaging, emerged as a way to address these difficulties. It recognizes images as data and mathematically extracts the spatial distribution of the pixel value and pixel-to-pixel relationships of the tissue in image through advanced mathematical analysis.⁴

Thousands of radiomics features can be obtained through various ways of mathematical formulas. Among them, histogram analysis is a distribution of gray-level frequency from the pixel intensity.

While histogram analysis does not consider the spatial interrelationships between gray values based on the location of the pixels,⁵ texture analysis is based on the pattern of pixel distribution. These features evaluate pixels in their local context, taking the relationship with adjacent pixels into account.^{5,6}

Until now, diagnosis of sialadenitis depends on the clinicians' subjective evaluation. However, it is expected that more objective diagnosis of sialadenitis can be achieved through these radiomics features.

Thus, in this study, based on the visual imaging evaluation of the gland in different inflammatory stage (normal, transient sialadenitis and chronic sialadenitis), the radiomics features in multi-imaging modality, CT, MR and US, were identified.

II. MATERIALS AND METHODS

1. Subjects

For experimental animals, a seven-week, 350-400-g western strain rat was used, which was kept under the same conditions (Nurturer: Orientbio Inc., Seongnam, Korea). All experimental processes were conducted with the approval of Yonsei University's ABMRC Experimental Animal Review. After the first week of conformity, it was classified into experimental groups (n=7) and control groups (n=8). Experimental workflow was described in Figure 1.

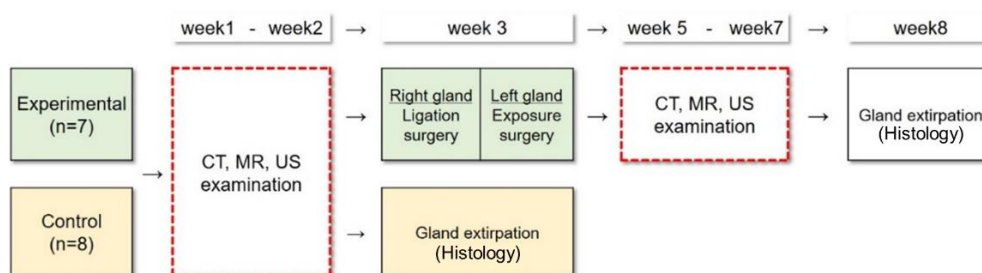


Figure 1. Schematic workflow of overall experiment (CT, computed tomography; MR, magnetic resonance imaging; US, ultrasonography)

2. Simulation of sialadenitis

For surgical simulation of sialadenitis, the experimental method was to inject a mixture of Ketamine (0.75 ml/kg) and Xylazine (0.15 mg/kg) into the selected size of the experimental group, wistar strain rat, into a general anesthesia. After hair removal, Betadine disinfection was performed on the neck area, 1cm horizontal incision of the central part was performed using surgical knives and scissors, and both subcutaneous lines were exposed. Find the right side of the gland and separate the blood vessels, then only the gland was bound using a suture (Silk 8/0, Ethicon Inc., Somerville, MA, USA) and then suture by a conventional method (Figure 2).

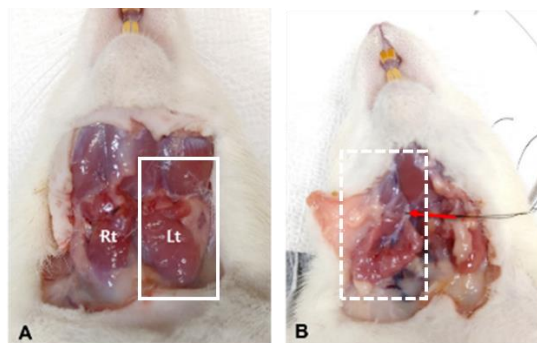


Figure 2. Surgical simulation of sialadenitis. A) Left submandibular gland (box) was exposed to induce transient sialadenitis. B) The ductal hilum (arrow) of right submandibular gland (dot box) was ligated to induce chronic sialadenitis.

The experiment was conducted in aseptic condition to prevent infection, and the pain medication meloxicam (2 mg/kg; Metacam, Boehringer Ingelheim, Germany) was injected to control the pain. During the experiment period, three experimental groups were raised together in a cage, and Animal feed and saline were allowed to be consumed freely.

3. Imaging acquisition and histologic examination

For all 15 subjects, contrast-enhanced CT, MRI and US were performed. Control subjects were sacrificed after imaging and glands were extirpated for histological examination. The experimental subjects underwent the same imaging examinations, contrast-enhanced CT, MRI and US, after 2 weeks from the surgery. We sacrificed and histologic examination. The equipment and imaging conditions are as follows (Table 1).

Table 1. Specification of unit and imaging condition according to the imaging modality

	CT	MR	US
Equipment	CosmoScan GX (Rigaku, Tokyo, Japan)	BioSpec94/20USR, 9.4 Tesla (Bruker BioSpin GmbH, Germany)	Vevo 2100 (FUJIFILM Sonosite- Visualsonics, Canada)
Imaging condition	Resolution, 140 μm ; tube voltage, 90 kV; tube current, 90 μA , scan time, 2 min; field-of- view, 70 mm	Fast spin echo T2 weighted images (FSE T2WI) - TR, 2750 ms; TE, 33 ms; FA, 90°; Field-of-view, 40x40 mm^2	Linear probe Center frequency, 21 MHz; gain, 18 dB; dynamic range, 65 dB; 3 points narrow focus; depth, 20 mm.
Contrast medium	Visipaque 320 (GE healthcare, US), 0.4 ml/kg		

4. Confirm of gland state

4.1 Imaging evaluation

Individual glands in all imaging modalities were evaluated by 1 radiologist and 1 surgeon of oral and maxillofacial specialty. In CECT, MRI and US, gland status was confirmed as normal, transient sialadenitis or chronic sialadenitis.

A) Normal gland: clear border with homogenous pattern

B) Transient sialadenitis: localized irregular border with loss of regular pattern in parenchyma

C) Chronic sialadenitis: indistinguishable border and heterogeneous parenchyma

All glands in experimental group before surgery and control group were confirmed as normal in CT, MRI and US. After the surgery, glands with exposure surgery only were confirmed as transient sialadenitis while glands with ligation surgery were confirmed as chronic sialadenitis (Figure 3).

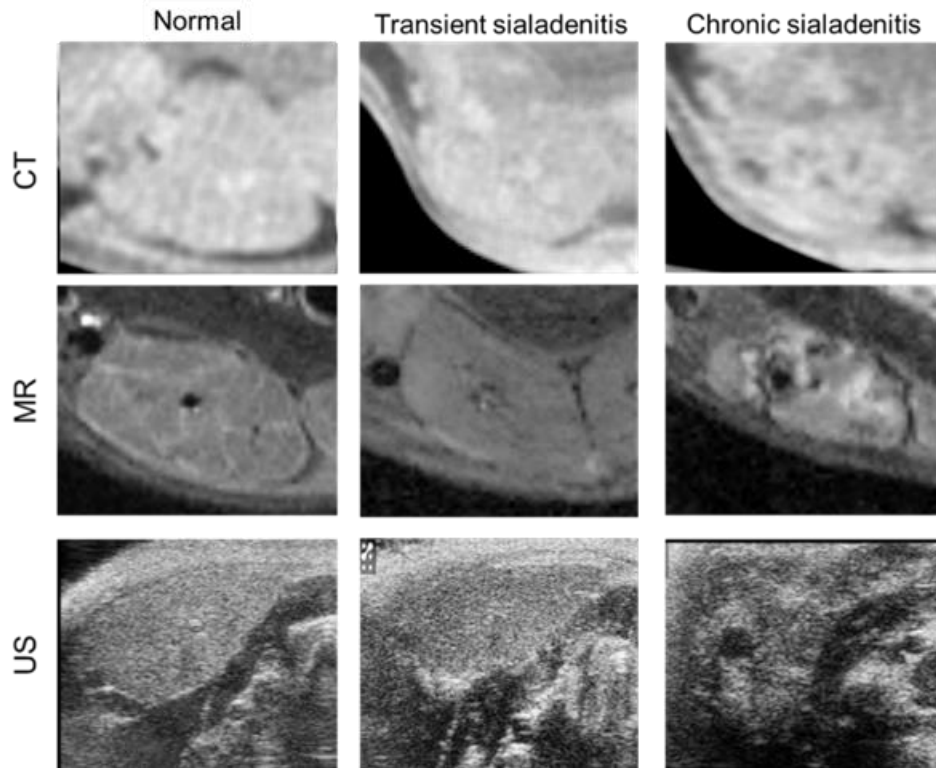


Figure 3. Representative image of normal gland, transient sialadenitis and chronic sialadenitis in CT, MR and US image (CT, computed tomography; MR, magnetic resonance imaging; US, ultrasonography).

4.2 Histological evaluation

Histology revealed a few inflammatory cells included locally in the gland of transient sialadenitis group. Whereas chronic sialadenitis group showed generalized infiltration of inflammatory cells and normal gland structure was destructed. Normal gland group showed no inflammation at all (Figure 4). This tendency was consistent with the trend of CT value and MR signal intensity measured based on the image.

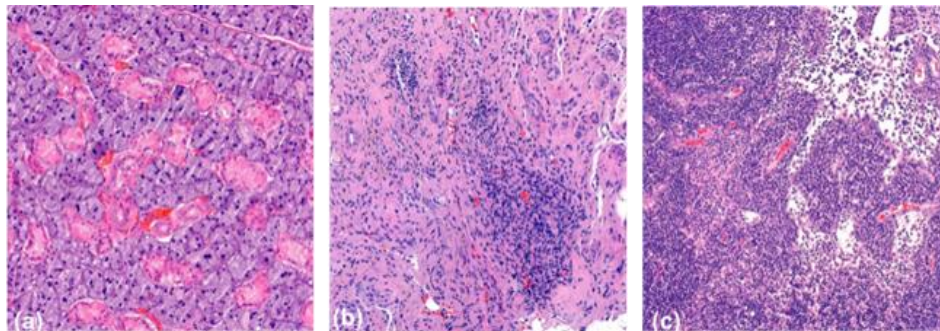


Figure 4. Histology presents (a) no inflammatory cells in normal gland, (b) local inflammatory cells in transient sialadenitis gland and (c) generalized inflammatory cells infiltration with destruction of gland structures (Hematoxylin & Eosin staining, x20)

5. Radiomics feature analysis according to gland state

For radiomics feature analysis, LIFEx version 7.0 (<https://www.lifexsoft.org>), a free open-source software developed as a tool to calculate radiomics data from the medical imaging.

In CT image, volume region of interest (ROI) was determined along with the border of individual gland. All axial, coronal, and sagittal sections were viewed on the software and only the gland region was selected (Figure 5A). For MRI and US, ROI was determined in the image showing the most area of the gland (Figure 5B, C). Within the selected ROI, the radiomics features obtained. The features obtained were total 50 features (first order :19, second and higher order: 31) we described in Table 2.

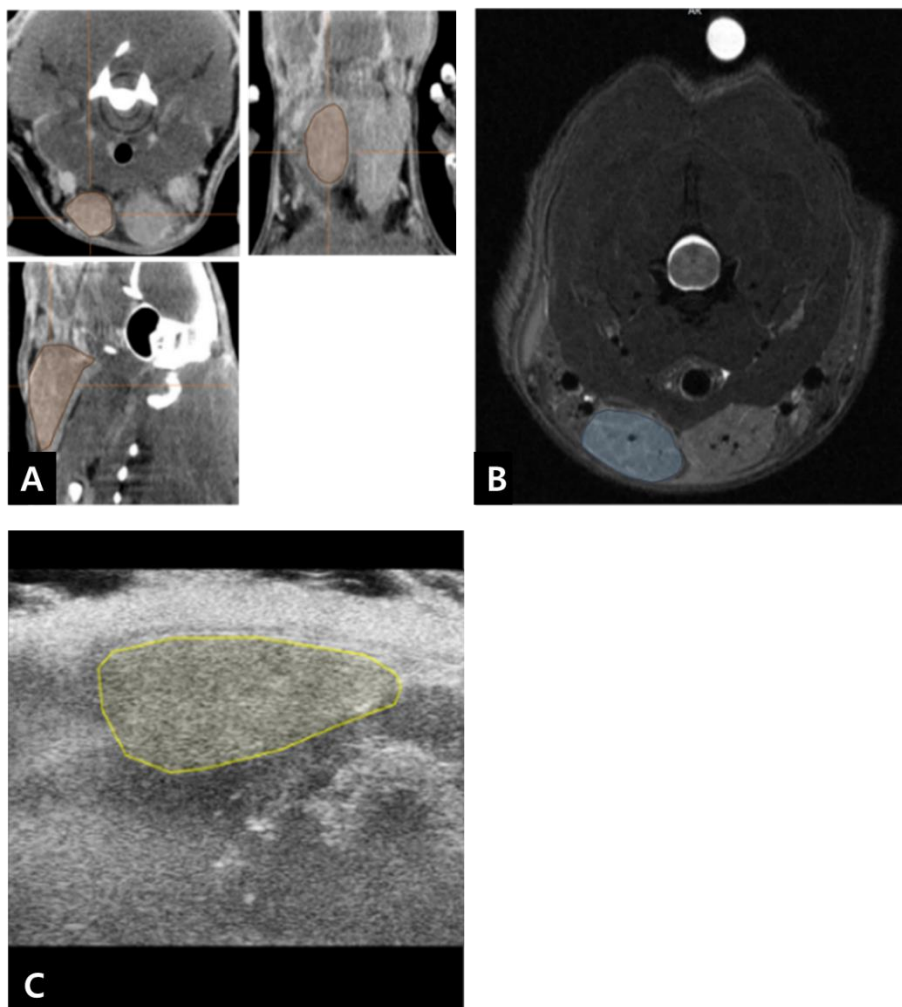


Figure 5. Region of interest (ROI) selection. A) 3-dimensional volume ROI is determined on submandibular gland in axial view of computed tomography. B) ROI is determined in the axial section of magnetic resonance imaging with gland most visible. C) ROI is determined along with the border of gland in ultrasonography.

Table 2. Overall radiomics features analyzed

First order	Histogram	Conventional		Discretized
	Skewness	HUmin		HUmin
	Kurtosis	HUmean		HUmean
	Entropy log10	HUsd		HUsd
	Entropy log2	HUmax		HUmax
	Energy	Q1		Q1
		Q2		Q2
		Q3		Q3
Second and higher order	GLCM	GLRM	NGLDM	GLZLM
	Homogeneity	SRE	Coarseness	SZE
	Energy	LRE	Contrast	LZE
	Contrast	LGRE	Busyness	LGZE
	Correlation	HGRE		HGZE
	Entropy	SRLGE		SZLGE
	Dissimilarity	SRHGE		SZHGE
		LRLGE		LZLGE
		LRHGE		LZLGE
		GLNU		GLNU
		RLNU		ZLNU
		RP		ZP

5. Statistical analysis

All radiomics values according to the gland state were compared using Kruskal willis test with 95% confidential interval. Post-hoc analysis was performed using Bonferroni test. Statistical test was conducted using SPSS (version 23, IBM Corporation, Armonk, NY, USA).

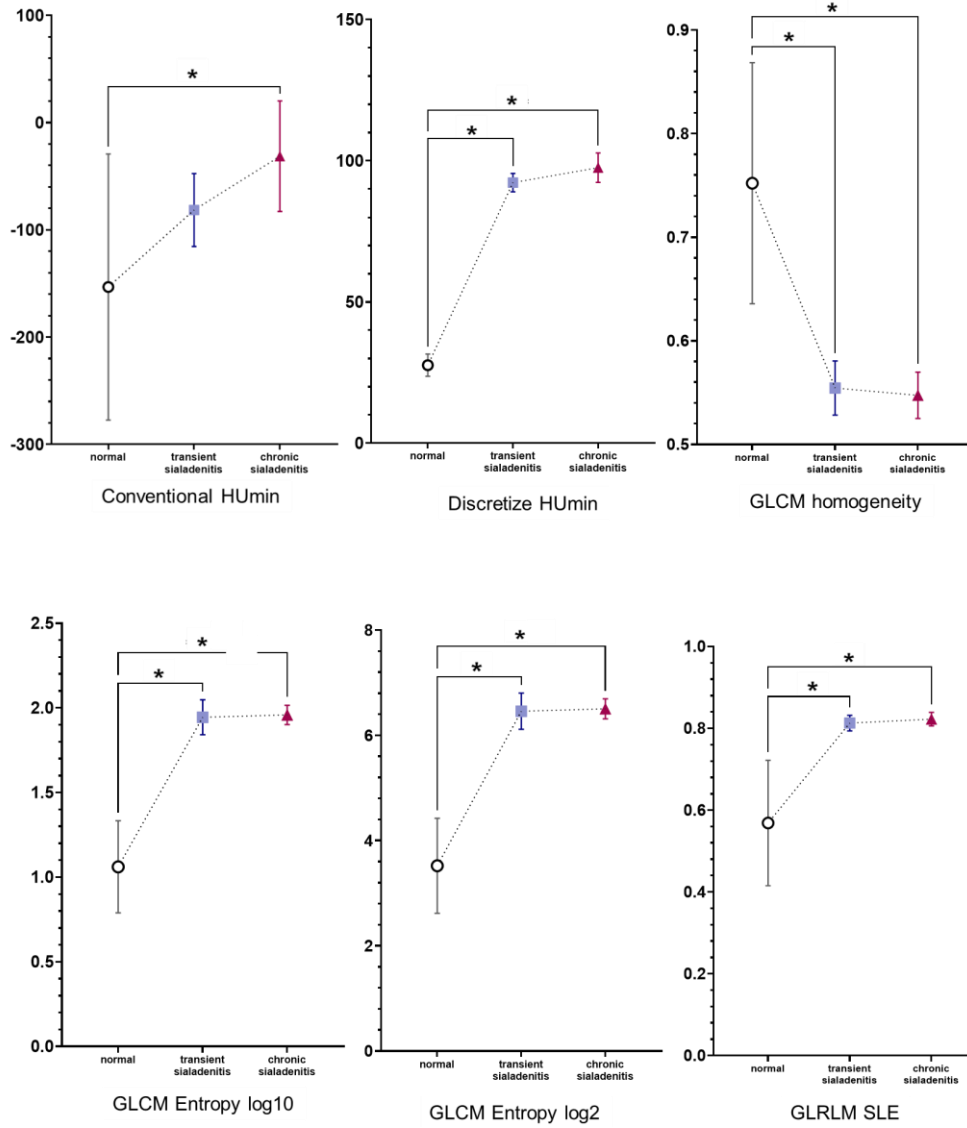
III. RESULTS

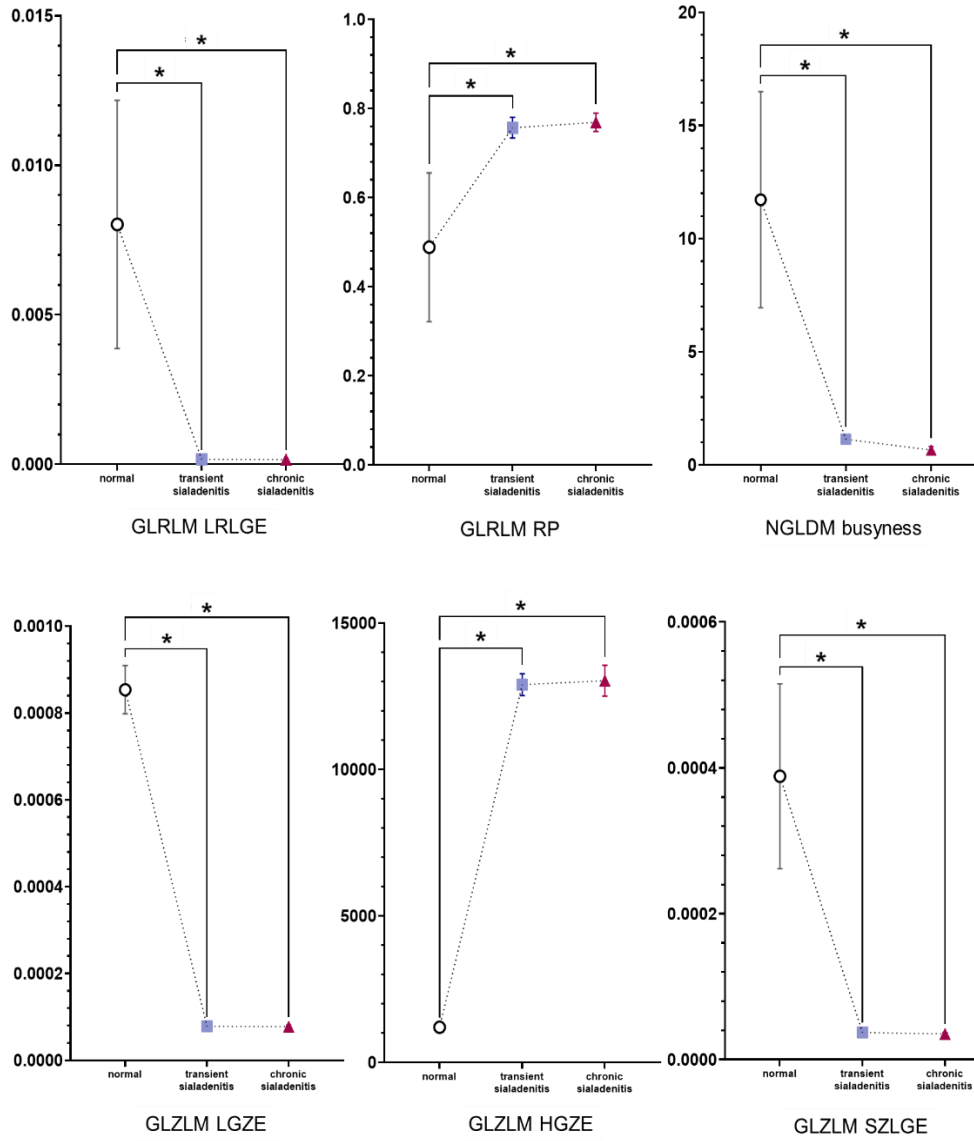
There were 13 radiomics features in CT, 9 in MRI, and 3 in US, showing statistical difference among gland status (Table 3).

All features of CT showed differences between normal and chronic sialadenitis groups. In the 12 features, there was also a significant difference between normal and transient sialadenitis groups. No variables showed any difference between the transient sialadenitis and the chronic sialadenitis group (Figure 6).

Table 3. Radiomics feature consistent with gland state

	CT	MR	US
Conventional	HUmin	HUmin HUQ1 HUskewness	HUstd
Discretize	HUmin	Q1 skewness	
GLCM	Homogeneity Entropy log10 Entropy log2		
GLRLM	SLE LRLGE RP	HGRE SRHGE	LRE
NGLDM	Busyness		
GLZLM	LGZE HGZE SZLGE LZLGE	HGZE SZHGE	LZE





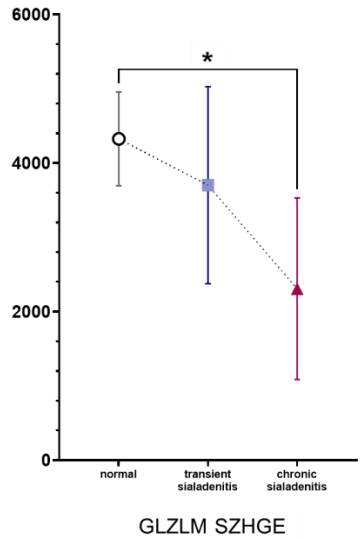
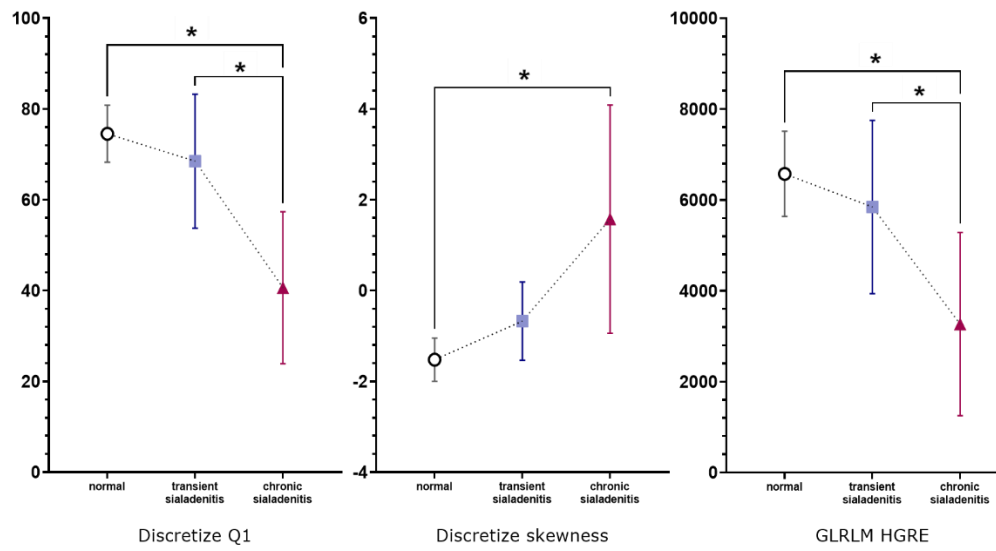
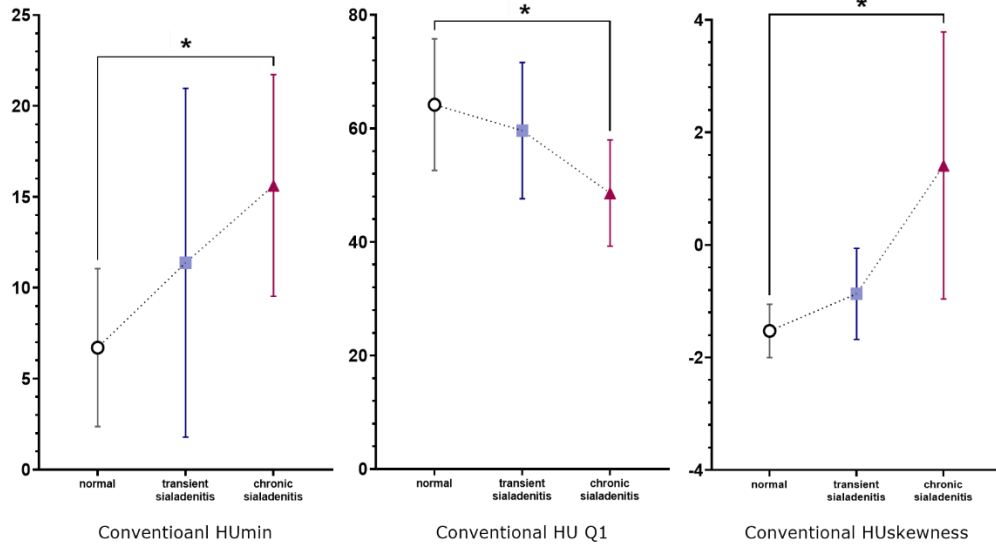


Figure 6. Features of computed tomography consistent with the standard value measurement (*P < 0.05)

MR also showed the difference between normal and chronic sialadenitis groups in all features selected. Unlike CT, MRI had four features that differed between transient and chronic sialadenitis groups, and no features that differed between normal and transient sialadenitis groups (Figure 7).



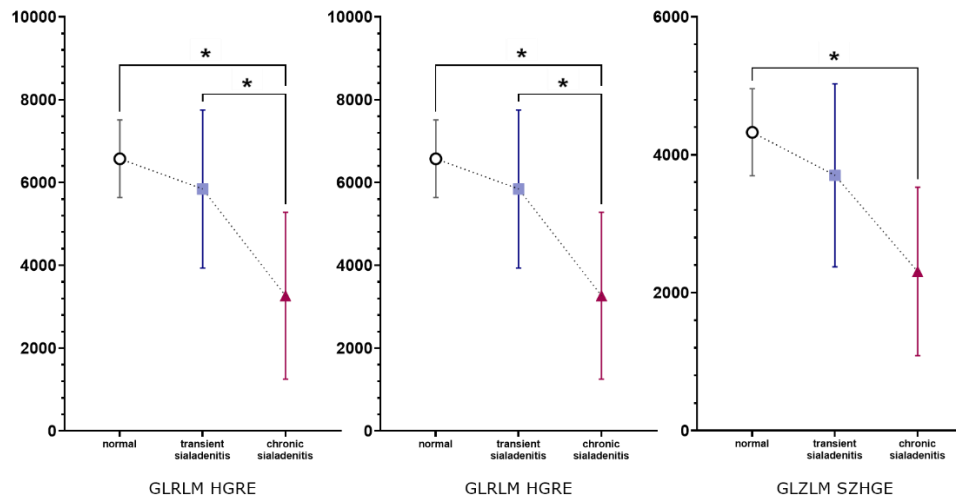


Figure 7. Features of magnetic resonance imaging consistent gland state measurement (* $P < 0.05$)

The features selected in the US also differed between normal and chronic sialadenitis groups, and in one feature, between transient and chronic sialadenitis groups (figure 8).

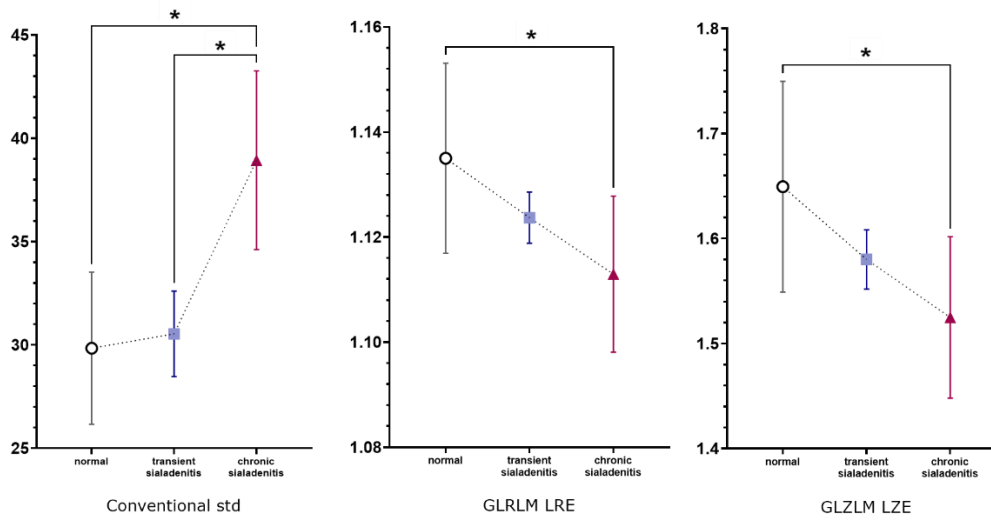


Figure 8. Features of ultrasonography consistent with gland state measurement
(*P < 0.05)

IV. Discussion

When inflammation of salivary gland occurs, acinar cells are gradually destroyed,⁷ stromal cells are replaced by fibrous connective tissue while ductal structures are dilated.⁸ The atrophy of the salivary gland progressed with proliferation of duct epithelium. In addition, vascular tissues proliferation is observed in salivary tissue.^{7,8} Serous gland showed more atrophy and destruction of tissue than mucous gland.⁸

In order to observe changes of gland structures in gross manner in imaging, contrast-enhanced CT or MRI is the modality of choice.^{4,9} The evaluation of gland in pathologic state based on these image modalities is more or less dependent on the clinician's decision. It has no choice but to depend on the clinician's experience or subjectivity. Thus, in this study, we attempted to provide objective decision criteria for sialadenitis via radiomics analysis of multiple imaging modalities.

Radiomics primarily emerged from the medical field of oncology and is

the most advanced in applications within that field.^{4,10,11} The hypothesis of radiomics is that the distinctive imaging features between disease forms may be useful for predicting prognosis and therapeutic response for various conditions, thus providing valuable information for personalized therapy. The analysis method extracts a large number of features from radiographic images based on pixel value using data-characterization algorithms. The extracted characteristics, termed as radiomics features, are expected to have the potential uncovering the innate of the disease, that fail to be appreciated by the naked eye.¹²

As a result of this study, there were several first-order features selected to differentiate normal and sialadenitis in CT, MR and US. In general, first-order features, which are derived from frequency histograms, lack any reference to the spatial interrelationship between gray values. Hence, although they provide useful information regarding the general shape of the gray-value distribution, first-order features are often supplemented by higher-order features.¹³ There were also various higher order features determined in all of 3 imaging modalities in the present study.

Such higher order texture analysis can be performed using one of three broad types of techniques: statistical, model-based, or transform-based. The statistical approach derives texture parameters from the frequency of occurrence of different gray values, and texture parameters are grouped on the basis of increasing complexity depending on the manner in which they represent the spatial relationship between gray values.¹³ Model-based approaches use mathematic models to derive textural properties from images. The transform-based approach converts the spatial information in an image into frequency (Fourier) information or into scale and frequency (wavelet) information.

This study showed multiple radiomics features presenting consistency with the visual assessment through CT, MRI and US. CT image showed most large number of features, followed by MRI. US showed the least number of features. Although US showed only 3 characteristics, the current study was meaningful as US showed applicability to detect sialadenitis and differentiate initial and chronic stage of sialadenitis.

Interestingly, many CT radiomics features showed statistical difference

between the normal and transient stage of sialadenitis. In contrast, MRI has many features differentiate normal gland from chronic sialadenitis with statistical significance. One possible explanation would be contrast medium was used for CT examination while it was not for MRI examination. Although MRI is choice of modality in soft tissue inflammatory lesion, it seemed that contrast medium played a large role much to enhance initial stage of gland inflammation. Further study can be suggested to obtain MRI under injection of gadolinium to subject.

On the other hand, characteristics which distinguished between transient and chronic sialadenitis were dominant in MRI and US. This was thought to be due to the imaging characteristic of MRI and US that they provide high definition of tissue with good signal-to-noise resolution. The contrast enhanced imaging may provide superior findings due to the blood flow increasing in the early stage of sialadenitis.¹⁴ However, it is presumed that the structural changes of the gland at the chronic stage of sialadenitis can be observed better with image with high resolution.

For diagnosing sialadenitis using US, the detection of the disease based

on the echogenicity is relatively subjective. Also, the criteria for sialadenitis diagnosis have not yet been established. Previous studies have reported an US imaging pattern in patients with progressing Sjogren's syndrome.¹⁵ They performed sequential US examination and sialography. The inter-observer consistency was studied between the two imaging modalities, and US showed comparable diagnostic ability with sialography. However, both US and sialography were difficult to make subjective diagnosis that the accuracy of both modality was limited to 75 - 80%. Therefore, the needs for subjective diagnostic criteria was absolutely necessary.¹⁰

To establish diagnostic criteria of US, quantification of echogenicity is essential. The texture features in radiomics was thought to be an appropriate and several features of US showed appropriateness. In this study, the HUstd, LRE, and LZE were selected as effective US features. HUstd is a type of scattering value that represents the degree of scattering of pixel values. The LRE (long run Emphasis) is the distribution of the long homogeneous runs of pixels in an image. The LZE (long zone emphasis) is

the distribution of the long homogeneous zones of pixels in the image.⁵ Those characteristics would be related with that as the sialadenitis progresses into chronic stage, the tissue became more heterogeneous and the intra-glandular ductules dilated.¹⁶ Thus, radiomics features of US may help to detect and follow-up inflammatory stage of salivary gland with relatively high objectivity without radiation exposure.

V. CONCLUSION

All imaging modality, CECT, MRI and US, showed radiomics characteristics showing consistency with gland state of sialadenitis. The radiomics characteristics of CT was superior to detect transient sialadenitis from normal gland. The characteristics of MRI and US showed better performance differentiating initial sialadenitis from chronic stage. This suggests that radiomics characteristics can be useful for recognizing the progression stage of sialadenitis based on the objective values. This study was also meaningful that it found useful US characteristics for recognizing the early and chronic sialadenitis. The US would be expected to be applied for both diagnosing and check-up imaging for sialadenitis.

REFERENCES

1. Nanci A. *Ten Cate's Oral Histology-e-book: development, structure, and function*: Elsevier Health Sciences; 2017.
2. Leake DL, Haydon GB, Laub D. The microscopy of parotid atrophy after ligation of Stensen's duct. *J Journal of Oral Pathology Medicine* 1974; **3**: 167-175.
3. Orlandi M, Pistorio V, Guerra P. Ultrasound in sialadenitis. *J Journal of ultrasound* 2013; **16**: 3-9.
4. Gillies RJ, Kinahan PE, Hricak H. Radiomics: images are more than pictures, they are data. *J Radiology* 2016; **278**: 563-577.
5. Lubner MG, Smith AD, Sandrasegaran K, Sahani DV, Pickhardt PJ. CT texture analysis: definitions, applications, biologic correlates, and challenges. *J Radiographics* 2017; **37**: 1483-1503.
6. Orlhac F NC, Buvat I. LIFEx manual Texture User Guide Local Image Features Extraction.
7. Atkinson JC, Fox PC. Salivary gland dysfunction. *J Clinics in geriatric*

- medicine* 1992; **8**: 499-512.
8. Abdel Razek AAK, Mukherji S. Imaging of sialadenitis. *J The neuroradiology journal* 2017; **30**: 205-215.
 9. Som PM, Curtin HD. *Head and Neck Imaging, 5th Edition*: Elsevier; 2011.
 10. Yip SS, Aerts HJ. Applications and limitations of radiomics. *J Physics in Medicine Biology* 2016; **61**: R150.
 11. Lambin P, Rios-Velazquez E, Leijenaar R, Carvalho S, Van Stiphout RG, Granton P, et al. Radiomics: extracting more information from medical images using advanced feature analysis. *J European journal of cancer* 2012; **48**: 441-446.
 12. Liu Z, Wang S, Di Dong JW, Fang C, Zhou X, Sun K, et al. The applications of radiomics in precision diagnosis and treatment of oncology: opportunities and challenges. *J Theranostics* 2019; **9**: 1303.
 13. Bashir U, Siddique MM, Mclean E, Goh V, Cook GJ. Imaging heterogeneity in lung cancer: techniques, applications, and challenges. *J American Journal of Roentgenology* 2016; **207**: 534-543.

14. Zenk J, Iro H, Klintworth N, Lell MJO. Diagnostic imaging in sialadenitis. *J Oral Maxillofacial Surgery Clinics* 2009; **21**: 275-292.
15. Takagi Y, Kimura Y, Nakamura H, Sasaki M, Eguchi K, Nakamura T. Salivary gland ultrasonography: can it be an alternative to sialography as an imaging modality for Sjögren's syndrome? *J Annals of the rheumatic diseases* 2010; **69**: 1321-1324.
16. Agni NA, Borle RM. Salivary gland pathologies: JP Medical Ltd; 2013.

국문요약

타액선염을 유발한 랫트의 다양한 영상에서
라디오믹스 분석을 통한 진단 기준 마련 연구

<지도교수 이채나>

연세대학교 대학원 치의학과

박군찬

연구목적: 본 연구는 타액선의 염증을 유발한 랫트의 전산화단층영상, 자기공명영상 및 초음파영상에서 라디오믹스 분석을 시행하여 타액선염을 진단하기 위해 적합한 특성값을 파악하고자 시행되었다. 특히, 초음파 영상에서 신뢰할 수 있으며 재현성 있는 변수를

확립하고자 한다.

연구대상 및 방법: 일정기간 동일 조건하에 사육된 7주, 350~400g 크기의 wistar strain 랫트를 1주일의 순응기간을 거친 뒤 실험군 7마리 및 대조군 8마리로 분류하였다. 모든 랫트에서 악하선 부위의 조영증강 전산화단층영상, T2 강조 자기공명영상 및 초음파영상을 획득하였으며, 이중 대조군은 희생하여 타액선을 적출하였다. 실험군은 목 부위를 절개하여 양측 악하선을 모두 노출하였으며, 우측 악하선의 분비관은 결찰 시행하여, 좌측 타액선은 일시적 염증, 우측은 만성 염증을 유발하였다. 2주 뒤 조영증강 전산화단층영상, T2 강조 자기공명영상 및 초음파영상을 획득하였으며 희생하여 악하선을 적출하였다.

획득된 모든 영상에서 1명의 영상치의학과 1명의 구강악안면외과 의사 합의하에 타액선 실질조직의 패턴을 육안으로 평가 시행하였다. 술 전 타액선이 모두 정상 패턴을 보이는지, 술 후 타액선이 일시적 혹은 만성적 타액선염 상태를 보이는 지 여부에 대해 평가하였다. 세 가지 상태의 타액선에 대해 조직학적으로 정상,

일시적 및 만성 타액선염을 확인하였다.

전산화단층영상, T2 강조 자기공명영상 및 초음파영상 모두에서 라디오믹스 분석을 위해 LIFE_x 소프트웨어에서 타액선의 경계를 따라 관심영역을 설정하였으며, 총 50개의 라디오믹스 특성에 대한 값을 획득하였다. 육안으로 평가된 결과와 일치하는 라디오믹스 특성을 추출하였다.

연구결과: 타액선 상태에 따라 통계학적으로 유의한 차이를 보이는 라디오믹스 특성은 전산화단층영상에서 13개, 자기공명영상에서 9개, 초음파에서 3개로 나타났다.

전산화단층영상의 13개 특성값은 모두 정상과 만성적 타액선염 사이에 유의한 차이를 보였다. 12개 특성에서는 정상과 일시적 타액선염 간에도 통계적으로 유의한 값의 차이를 보였다. 자기공명영상의 경우에도 9개 특성 모두 정상과 만성적 타액선염 간 차이를 보였으며, 이 중 4개의 특성에서는 일시적 타액선염과 만성적 타액선염 사이에도 값의 유의한 차이가 있었다. 초음파영상에서 선별된 변수들 역시 정상과 만성적 타액선염 간 차이가 있었으며, 이

중 1개의 특성에서는 일시적 및 만성적 타액선염 간에도 차이를 보였다.

연구결론: 각각의 영상에서 모두 CT 값 및 T2 신호강도 분석과 유사한 경향성을 보이는 라디오믹스 특성값을 찾을 수 있었다. 특히, 전산화단층영상의 경우 정상과 일시적 타액선염 사이에 유의한 차이를 보이는 특성값이 다수 존재하였는데, 이는 초기 염증 진단에서 전산화단층영상이 유리할 수 있음을 보여준다. 또한, 자기공명영상 및 초음파영상의 경우 일시적 타액선염과 만성적 타액선염 사이에 유의한 차이를 보이는 특성이 있었다. 이는 염증의 진행 상황과 단계별 구분에 유용할 수 있음을 시사한다. 본 연구를 통해 초음파영상의 라디오믹스 특성 분석을 통한 타액선염의 진단 및 추적 검사에 적용 가능성을 알 수 있다.

핵심어: 라디오믹스, 타액선염, 전산화단층영상, 자기공명영상, 초음파영상